Transmural Heterogeneity in Ion Channel Properties in the Left Ventricle Optimizes Pump Function during Natural Electrical Activation

E Hermeling[1], TM Verhagen[2], FW Prinzen[1], NHL Kuijpers[1]

[1]Maastricht University, Maastricht, The Netherlands
[2]Eindhoven University of Technology, Eindhoven, The Netherlands

Abstract

In this simulation study, we hypothesize that transmural heterogeneity in ion channel properties serves to homogenize cardiac workload. Mechanics and electrophysiology were modeled both on cellular and tissue level. Endo-, midmyo- and epicardial cells differed in ion channel properties only. A preload-afterload experiment was simulated to analyze cardiac pump function during normal conduction from endo to epicardium (activation delay = 26 ms). For a homogeneous distribution, insufficient afterload (epi- or endocardial cells only) or increased diastolic stress (midmyocardial cells only) was observed. Simulating 50% midmyocardial cells, we observed the most homogenous distribution of workload, when midmyocardial cells were shifted towards the endocardium. We conclude that transmural heterogeneity in electrophysiology is essential for proper diastolic and systolic function and for a uniform distribution of workload across the ventricular wall.

1. Introduction

In multiple studies, transmural differences in electrophysiological properties in the left ventricular wall have been observed [1,2]. The consequence of this heterogeneity for cardiac pump function is, however, poorly understood. In this study, we hypothesize that heterogeneity in electrophysiology serves to homogenize cardiac workload, using a model that describes both electrophysiology and mechanics. An extended preload-afterload experiment was simulated to model the cardiac cycle. Simulations were performed using either homogenous or heterogeneous fibers composed of endo-, midmyo- and epicardial cells.

2. Methods

The 1D model represents a tissue with a length of 10 mm, composed of 100 segments with a cross-sectional area of 0.1 mm^2 each. Electrophysiology and mechanics were described on cellular as well as tissue level, see Figure 1.
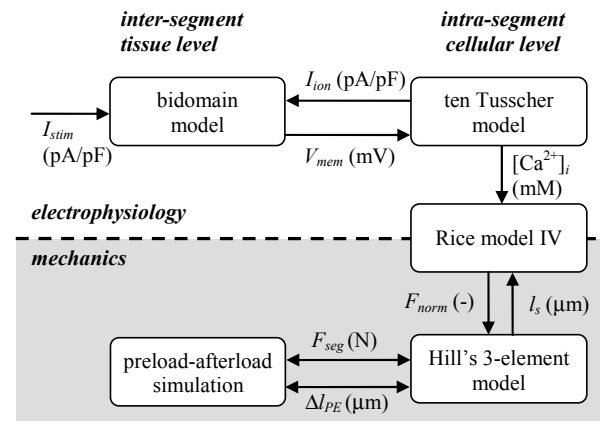

Figure 1. Schematic overview of the simulation model. On cellular level, electrophysiology, excitation-contraction coupling and mechanics are described by ten Tusscher [5], Rice IV [6] and Hill's 3-element model [4,7,8], respectively. Electrical interaction on tissue level is described by the Cellular Bidomain Model [3, 4]. Mechanically, Hill's models are placed in series [9] and subjected to a preload-afterload simulation [10].

2.1. Electrophysiology

On tissue level, electrophysiology is simulated by the Cellular Bidomain Model [3,4]. Each segment is defined by the intracellular (V_{int}), extracellular (V_{ext}), and membrane potential ($V_{mem} = V_{int} - V_{ext}$). Exchange between the intracellular and extracellular domains occurs as transmembrane current (I_{trans}) consisting of an ionic current (I_{ion}) and a capacitive current:

$$I_{trans} = \chi \left(C_{mem} \frac{dV_{mem}}{dt} + I_{ion} + I_{stim} \right), \qquad (1)$$

where, $\chi = 2000$ cm^{-1} is the surface area to volume ratio of the tissue, $C_{mem} = 1.0\,\mu F/cm^2$ is the membrane capacitance. To initiate a depolarization wave, the

segment at 0 mm was stimulated with I_{stim} = -100 pA/pF. Segments were electrically connected with intracellular (g_{int} = 1.74 mS/cm) and extracellular conductivity (g_{ext} = 6.25 mS/cm).

To model the ionic membrane current (I_{ion}), the model of ten Tusscher et al. [5] was applied, describing all relevant ionic membrane currents, each related to V_{mem}. Calcium dynamics were described by four compartments i.e. extracellular space, cytoplasm, sarcoplasmatic reticulum and dyadic subspace and included buffering of Ca^{2+}.

Transmural differences in electrophysiology between endo-, midmyo-, epicardial cells and their intermediates were modeled by varying the transient outward current (I_{to}) and the slow rectifier current (I_{Ks}). This resulted in a longer action potential duration and consequently longer calcium transient duration and elevated intracellular calcium concentration ($[Ca^{2+}]_i$) in midmyocardial cells compared to the endo- and epicardial cells.

2.2. Excitation-contraction coupling

To describe the excitation-contraction coupling, the fourth model of Rice [6] is fed with $[Ca^{2+}]_i$ from the ten Tusscher model. This model includes the dynamics of troponin binding to Ca^{2+} and non-permissive (N) and permissive (P) states of cross-bridges (XBs). A XB can be either unbound (N_0, P_0) or bound (N_1, P_1, P_2, P_3), with a maximum of 3 XBs. The model includes two cooperative mechanisms of cardiac muscle: 1) the attachment of a XB increases the rate of formation of new XBs and 2) the binding of Ca^{2+} to troponin facilitates the transition of XBs to the permissive state. The contractile force (F_{norm}) of is determined by:

$$F_{norm} = \alpha \left(N_1 + P_1 + 2P_2 + 3P_3 \right), \qquad (2)$$

where N_1, P_1, P_2 and P_3 denote the fractions in the corresponding state (depending on sarcomere length (l_s) and $[Ca^{2+}]_i$) and α the fraction of thick filament in single overlap as determined by l_s.

2.3. Mechanics

Each segment is described by Hill's 3-element model [8], in which the force of the contractile element (F_{CE}) is determined by F_{norm}, obtained from the Rice model, a material constant (f_{CE} = 100 kPa) and the Hill's force velocity relation $f_v(v)$ [7] by:

$$F_{CE} = f_{CE} f_v(v) F_{norm}\left([Ca^{2+}]_i, l_s\right), \text{ with} \qquad (3)$$

$$f_v(v) = \frac{1 - v/v_{max}}{1 + c_v(v/v_{max})}, \qquad (4)$$

where, $v = dl_s/dt$ is the velocity of sarcomere shortening, v_{max} = 5.5 µm/s is the maximal velocity and c_v = 2 is a constant describing the shape of the hyperbolic

function. The total force of the 3-element model (F_{seg}) is the sum of the serial ($F_{SE} = F_{CE}$) and parallel elastic (F_{PE}) force approximated by an exponential relation.

$$F_{seg} = f_{SE} \exp\left(k_E l_{SE}\right) + f_{PE} \exp\left(k_E l_{PE}\right), \qquad (5)$$

where, l_{SE} and l_{PE}, are the lengths of the series and parallel element, (note: $l_{PE} = l_{SE} + l_s$); the material constants are defined as f_{SE} = 28 kPa, f_{PE} = 6 Pa, and k_E = 14.6 µm^{-1} [4].

The left ventricular cavity may be considered as a single myofiber, starting from the epicardium at the base and spiraling down to the apex, from which it spirals back to the endocardium at the base. Therefore, left ventricle dynamics may be approximated by single fiber strain and stress [9], with endo-, midmyo-, and epicardial cells connected in series. Fiber stress and strain were calculated for isotonic as well as isometric conditions as described in detail before [3].
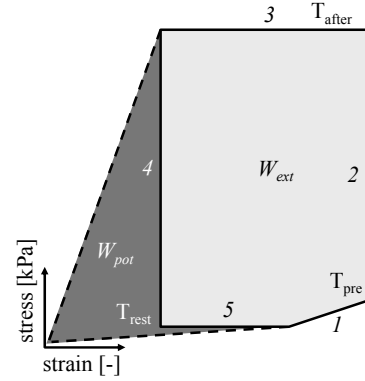
Figure 2. Overview of simulated preload-afterload experiment, see text for details. External (W_{ext}) and potential work (W_{pot}) are defined by the light and dark grey areas, respectively.

2.4. Preload-afterload experiment

To simulate the cardiac cycle, the total fiber is subjected to an extended preload-afterload experiment [10], according to following protocol (see Figure 2).
1. Filling phase, linear increase in stress towards preload stress (T_{pre} = 1.5 kPa);
2. Isovolumic contraction phase, isometric contraction until afterload stress is reached (T_{after} = 10 kPa);
3. Ejection phase, isotonic contraction until total fibers strain stops decreasing;
4. Isovolumic relaxation phase, isometric relaxation until resting stress is reached (T_{rest} = 0.75 kPa);
5. Isotonic relaxation until filling phase starts.

2.5. Simulation and data analysis

We refer to [4] for the numerical scheme. To ensure a steady state response, we performed simulations of

50 s, using seven fiber compositions (Figure 3):
1. Homogenous, consisting only of endocardial cells (1a), midmyocardial cells (1b), epicardial cells (1c);
2. Gradual change in ion channel properties from epi- toward endocardium;
3. Majority midmyocardial cells (50%) located in the center of the ventricular wall (3a) or shifted towards endo- (3b) or epicardium (3c);
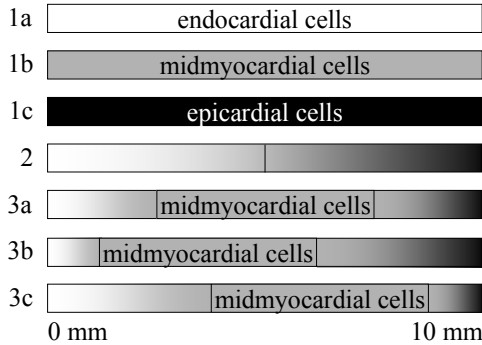
Figure 3. Seven fibers composed of endo-, midmyo-, and epicardial cell types (see text for details).

We analyzed the simulations of the different fiber compositions, on external (W_{ext}) and total ($W_{tot} = W_{ext} + W_{pot}$) work as defined in Figure 2. Moreover, we analyzed heterogeneity (dispersion) of strain ($\varepsilon = \Delta l_{PE}/l_{PE,0}$) and work over the segments based on the variation coefficient (CV = standard deviation / mean).

3. Results

All simulations had an activation delay of about 26 ms between endo- and epicardium, corresponding to an electrical conduction velocity of 0.4 m/s. Moreover, all segments had a similar electromechanical delay and, hence, propagation velocity of start of contraction (defined as $F_{norm} > 0$) was 0.4 m/s as well. The propagation velocity of onset of myofiber shortening (0.1 m/s) was slower than the electrical conduction and start of contraction velocity.

In simulation 1a and 1c (endo- or epicardial cells only), the stress developed by the sarcomeres was too low to reach T_{after}. In simulation 1b (midmyocardial cells) T_{rest} was not reached to complete the cardiac cycle.

Compared to a gradual change in ion channel properties from endo- to epicardium (2), a majority of midmyocardial cells in the center of the tissue (3a), led to an increase in total work of 1.13 to 1.33 kJ/m³ and external work of 0.31 to 0.68 kJ/m³ (Table 1). A shift of the midmyocardial cells towards epi- and endocardium resulted in a 3% lower and 8% higher external work, respectively, as compared to 3a.
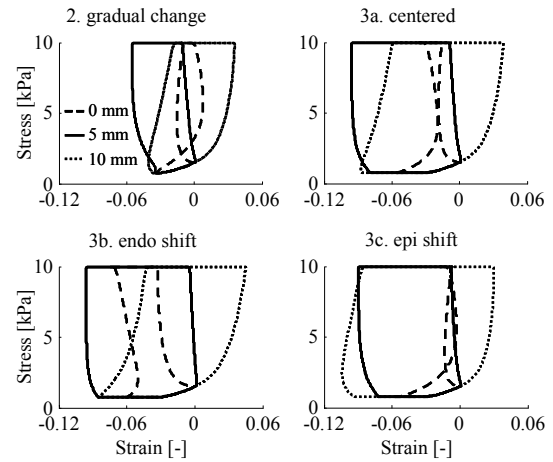
Figure 4, Stress-strain loops in four heterogeneous fiber compositions (see text for details).

Figure 4 shows the stress-strain loops of three segments at 0 mm (endocardium), 5 mm and 10 mm (epicardium) for the heterogeneous fiber compositions. Except for the endocardial shift (3b), very small or negative external work was observed at the endocardium. In accordance with this observation, a large dispersion in external work (CV_{Wext}) was observed between the individual segments in simulations 2, 3a and 3c (Table 1). Endocardial shifting of midmyocardial cells (3b) showed a more homogeneous distribution of workload.

Table 1, Workload and dispersion of workload and strain for each of four heterogeneous fiber compositions

	2. gradual	3a. centered	3b. endo shift	3c. epi shift
W_{ext} (kJ/m³)	0.31	0.68	0.73	0.66
W_{tot} (kJ/m³)	1.13	1.33	1.36	1.32
CV_{Wext} (%)	82	48	29	63
$CV_{\varepsilon max}$ (%)	12	19	16	28

The maximal normalized dispersion in strain ($CV_{\varepsilon max}$) was lowest for endocardial shift (3b) compared with midmyocardial cells located near epicardium or the center of the wall (Table1, Figure 5).

4. Discussion and conclusions

Simulation results from this relatively simple model indicate that the observed transmural difference in electrical properties of myocytes, with increased action potential duration in the left ventricular midwall [1,2], may help to obtain a more uniform distribution of work across the left ventricular wall. Moreover the results suggest that differences in myocyte phenotype over the left ventricular wall is essential to 1) be able to develop

sufficient force, attributed to the midmyocardial cells that have elevated intracellular calcium concentration, and 2) relax quickly enough, attributed to epicardial cells that have a relative short calcium transient duration.
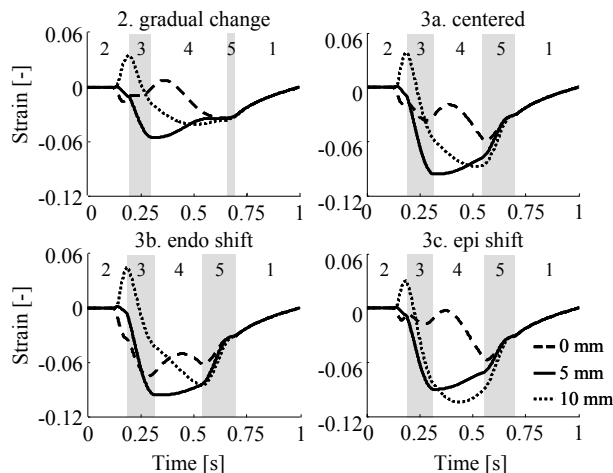

Figure 5, Strain curves of four heterogeneous fiber compositions (see text for details).

Experimental studies in canine showed that the highest duration in calcium transient [1] and action potential [11] was observed near the endocardium. This is in agreement with our observation that a better distribution of workload and strain is observed when cells with elongated action potentials and calcium transients are located close to the endocardium.

The relative large difference in electrical conduction velocity and propagation velocity of myofiber shortening observed in this study corresponds well with in vivo findings [12]. Our simulations suggest that this phenomenon can be explained by mechanical interaction of myocytes placed in series rather than difference in electromechanical delay between endo- and epicardial cells, as is suggested by others [12].

Our simulations results suggest that ventricular pump function benefits from heterogeneous electro-physiological properties across the ventricular wall. It remains, however, to be determined whether midmyocardial cells exist as a distinct differentiated cell type (M-cells) or these differences are the consequences of mechano-electrical adjustment to get a more homogeneous workload or strain.

We conclude that midmyocardial cells serve to apply sufficient work, whereas, especially, epicardial cells are needed to optimize diastolic function of cardiac muscle. Our simulations suggest that heterogeneity in electrophysiology helps to homogenize cardiac workload as seen in an endocardial shift of

midmyocardial cells; in this simulation a close to homogeneous distribution of workload and strain was observed as well as an increased amount of total and external work.

References

[1] Laurita KR, Katra R, Wible B, Wan X, Koo MH. Transmural heterogeneity of calcium handling in canine. Circ Res 2003;92: 668-75.

[2] Cordeiro JM, Greene L, Heilmann C, Antzelevitch D, Antzelevitch C. Transmural heterogeneity of calcium activity and mechanical function in the canine left ventricle. Am J Physiol Heart Circ Physiol 2004;286 H1471-9

[3] Kuijpers, NHL, ten Eikelder HM, Bovendeerd PHM, Verheule S, Arts T, Hilbers PAJ. Mechanoelectric feedback leads to conduction slowing and block in acutely dilated atria: a modelling study of cardiac electromechanics. Am J Physiol Heart Circ Physiol 2007;292: H2832-53

[4] Kuijpers NHL, ten Eikelder HM, Bovendeerd PHM, Verheule S, Arts T, Hilbers PAJ. Mechanoelectric feedback as a trigger mechanism for cardiac electrical remodeling: a model study. Ann Biomed Eng 2008;36:1816-35.

[5] Ten Tusscher KH, Panfilov AV. Alternans and spiral breakup in a human ventricular tissue model. Am J Physiol Heart Circ Physiol 2006;291:H1088-100.

[6] Rice JJ, Winslow RL, Hunter WC, Comparison of putative cooperative mechanisms in cardiac muscle: length dependence and dynamic responses. Am J Physiol 1999;276:H1734-54.

[7] Hill AV. The heat of shortening and the dynamic constants in muscle. Proc Roy Soc London 1938; 126:136-95

[8] Hunter PJ, McCulloch AD, ter Keurs HEDJ. Modelling the mechanical properties of cardiac muscle. Progr Biophys Mol Biol 1998;69:289-331.

[9] Arts T, Bovendeerd P, Delhaas T, Prinzen F. Modeling the relation between cardiac pump function and myofiber mechanics. J Biomech 2003 36;731-6.

[10] Brutsaert DL, Sonnenblick EH. Nature of the force-velocity relation in heart muscle. Cardiovasc Res;1961:1:suppl 1:18-33

[11] Verduyn SC, Jungschleger JGM, Stengl M, Spätjens RLHMG, Beekman JDM, Vos MA. Electrophysiological and proarrythmic parameters in transmural canine left-ventricular needle biopsies. Eur J Physiol 2004;449:115-22

[12] Ashikaga H, Coppola BA, Hopenfield B, Leifer ES, McVeigh ER, Omens JH. Transmural dispersion of myofiber mechanics. J Am Coll Cardiol 2007;49:909-16

Address for correspondence

Nico Kuijpers
Biomedical Engineering, CARIM, Maastricht University
P.O. Box 616, 6200 MD Maastricht, Netherlands
nico.kuijpers@bf.unimaas.nl